

Conformational toggling controls target site choice for the heteromeric transposase element Tn7

Qiaojuan Shi^{1,3,#}, Marco R. Straus^{1,#}, Jeremy J. Caron², Huasheng Wang², Yu Seon Chung², Alba Guarné^{2*} and Joseph E. Peters^{1*}

The supplementary material contains nine Supplementary Figures and one Table:

Supplementary Figure S1: Characterization of the N- and C-terminal domains of TnsE

Supplementary Figure S2: The C-terminal domain of TnsE has a novel fold.

Supplementary Figure S3: Electron density of the V-loops for the 12 TnsE-CTD molecules in the asymmetric unit.

Supplementary Figure S4: Fitting of the alternate conformations of the V-loop in an averaged composite omit map.

Supplementary Figure S5: Packing environment of the TnsE-CTD asymmetric unit.

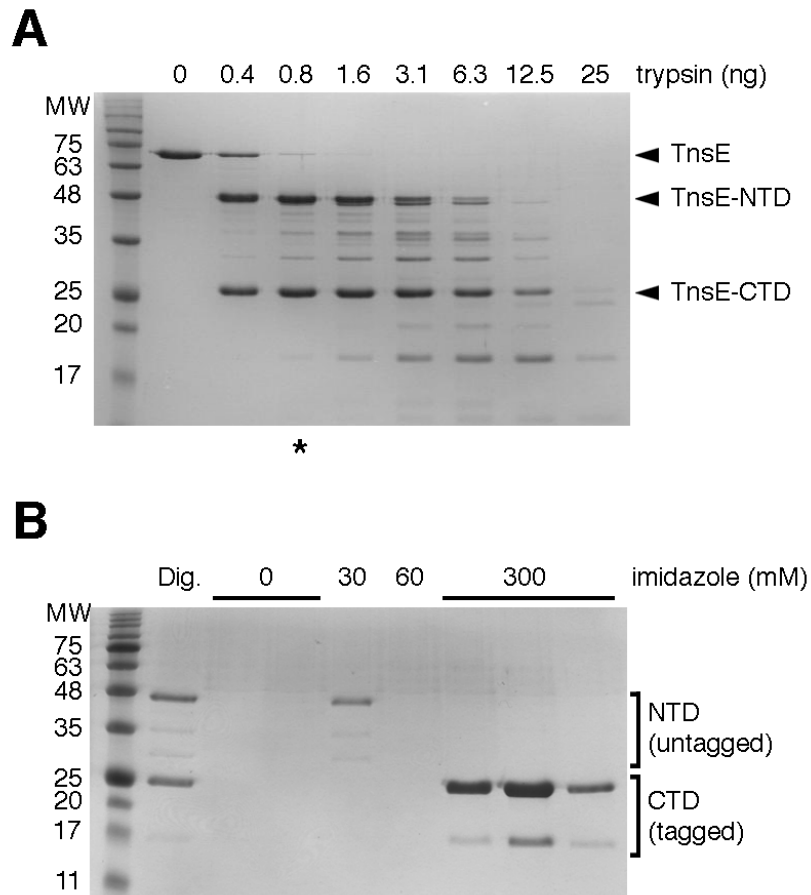
Supplementary Figure S6: Molecular replacement and composite omit map of the TnsE-CTD^{AVDN} structure.

Supplementary Figure S7: *In vivo* transposition activity of the A453T allele in the context of various other mutant alleles.

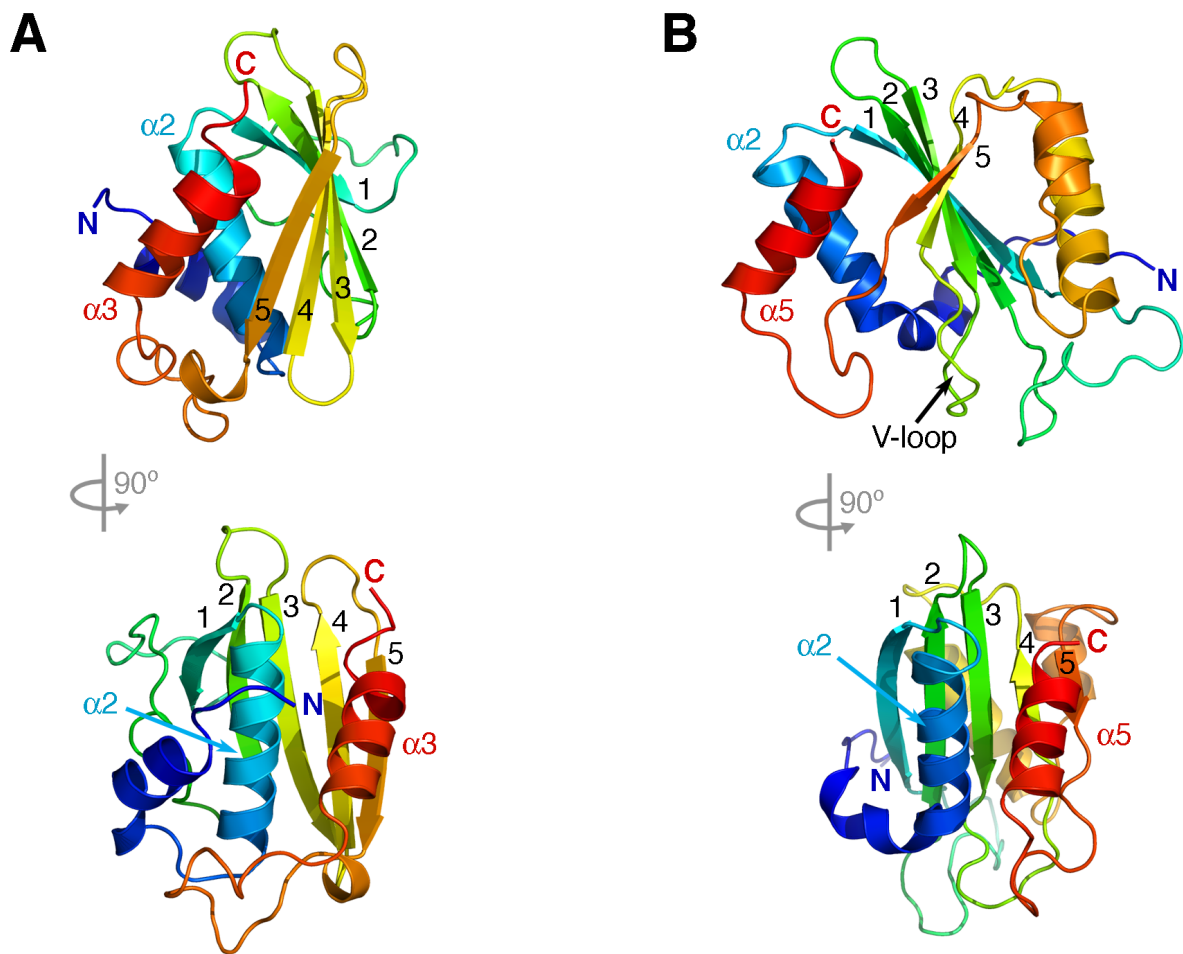
Supplementary Figure S8: Distribution of tn7 insertions across the *E. coli* chromosome in various genetic backgrounds.

Supplementary Figure S9: Model for DNA target discrimination by TnsE.

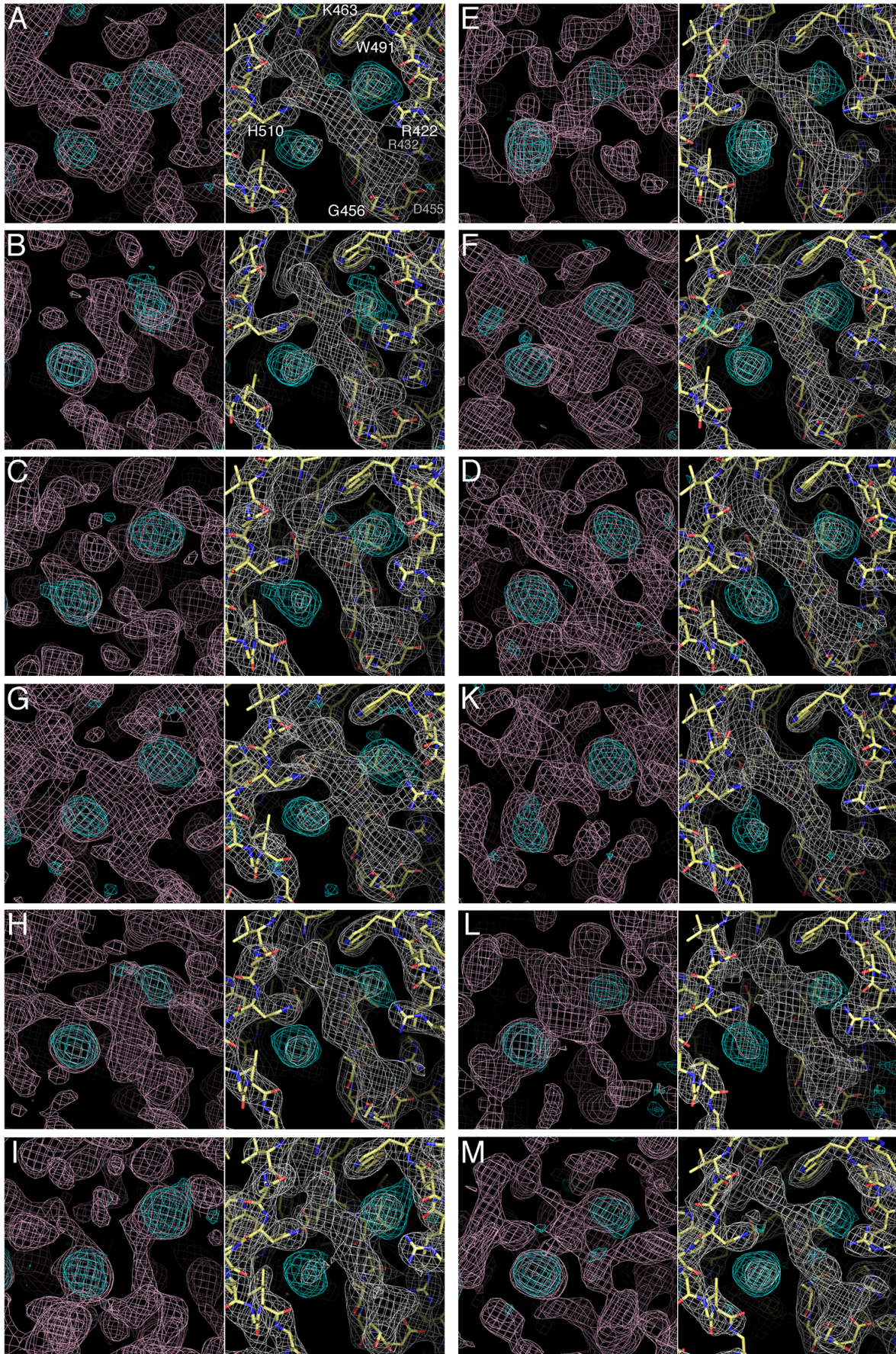
Table S1: Transposition activity in the TnsE single amino acid change mutants.



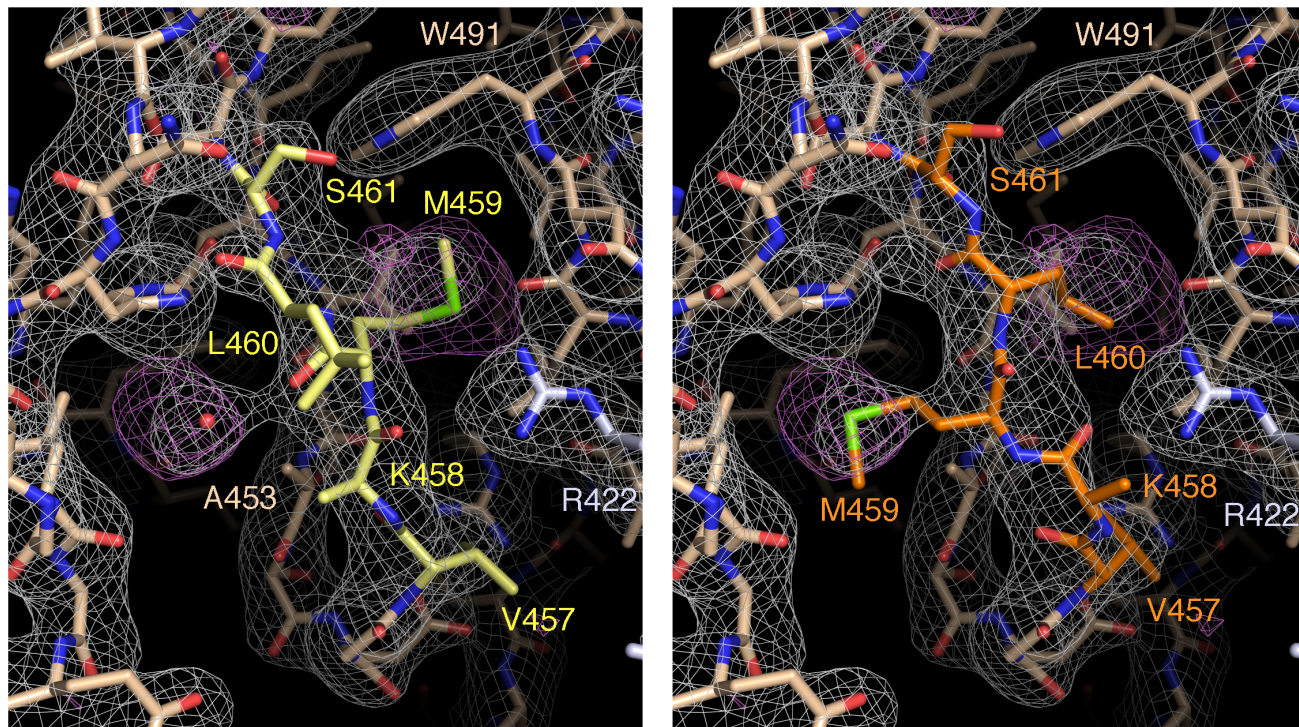
Supplementary Figure S1: Characterization of the N- and C-terminal domains of TnsE. (A) TnsE (12 μ g) was incubated with increasing concentrations of trypsin (0.4-25 ng) and the digestion products were resolved over 12% SDS polyacrylamide gels. Molecular weight markers are indicated in kDa. The digestions conditions used for the large-scale digestion are indicated with an asterisk. (B) Purification of the digestion products over a Ni-affinity chromatography column. The digestion reaction (labeled Dig.) was loaded onto a Ni-affinity column. The column was subsequently washed with increasing concentrations of imidazole (30, 60 mM) to remove untagged digestion products, prior to elution of the tagged digestion products with 300 mM imidazole. Purified TnsE includes a non-removable C-terminal hexa-histidine tag, therefore retained products correspond to the C-terminal domain of the protein.



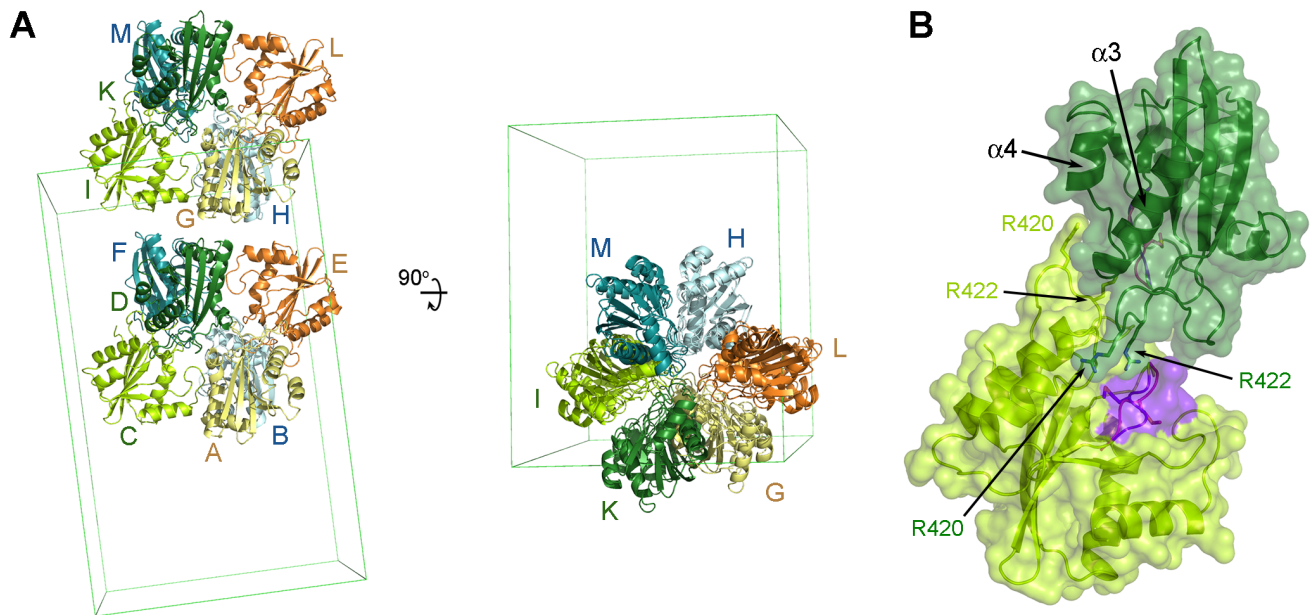
Supplementary Figure S2: The C-terminal domain of TnsE has a novel fold. (A) Orthogonal view of PI31 (PDB: 2VT8). (B) Orthogonal view of TnsE-CTD. Structures shown as rainbow ribbons colored from blue (N-terminus) to red (C-terminus). The shared secondary structure elements, as well as the position of the V-shaped look (V-loop) of TnsE, are labeled.



← **Supplementary Figure S3: Electron density around the V-loops for the twelve TnsE-CTD copies in the asymmetric unit.** The experimental (pink, 1σ) and composite omit (white, 1σ) electron density maps around the V-loop are shown side by side for each TnsE-CTD molecule in the asymmetric unit (ASU). The anomalous map (cyan, 3σ) is shown in both panels. The refined TnsE-CTD model is shown in the right-hand side panels with the alternate conformations excluded for clarity. Panels are labeled A-M corresponding to the chain ID of each molecule in the ASU.

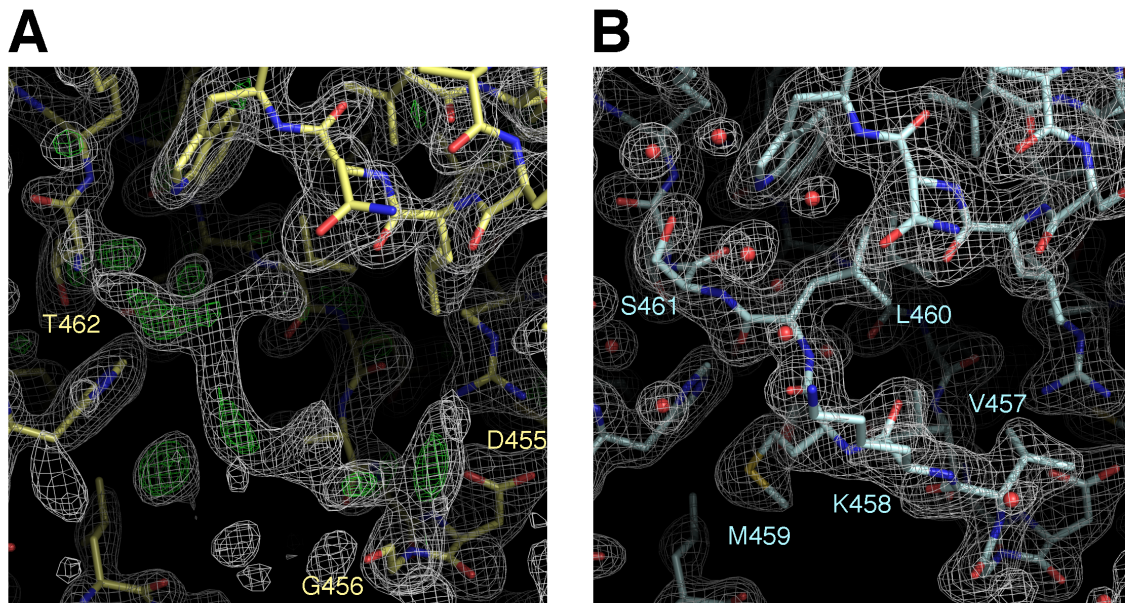


Supplementary Figure S4: Fitting of the alternate conformations of the V-shaped loop in an averaged composite omit map. The refined TnsE-CTD model (molecule A) is shown as tan color-coded sticks with the alternate conformations of the V-shaped loop shown in yellow and orange, respectively. The averaged composite omit (contoured at 1σ) and the experimental anomalous (contoured at 3σ) electron density maps are shown as white and purple meshes, respectively. Neighbouring molecules are shown as blue color-coded sticks.

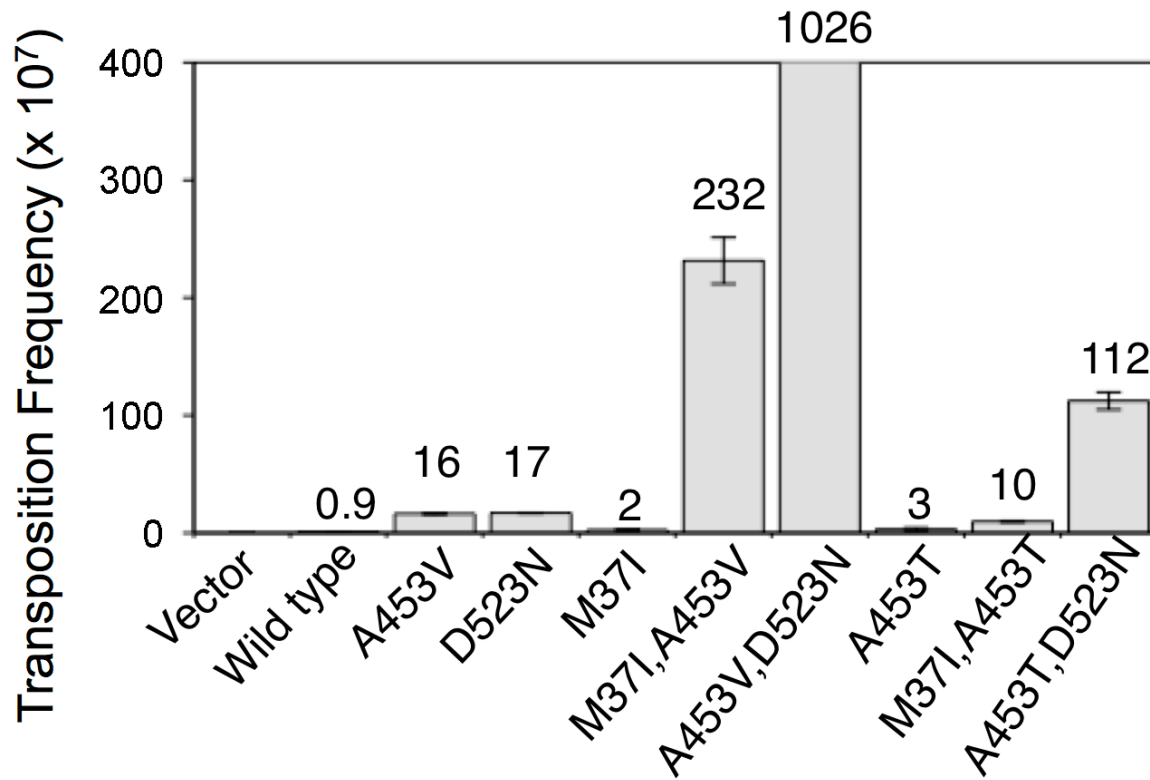


Supplementary Figure S5: Packing environment of the TnsE-CTD asymmetric unit. (A)

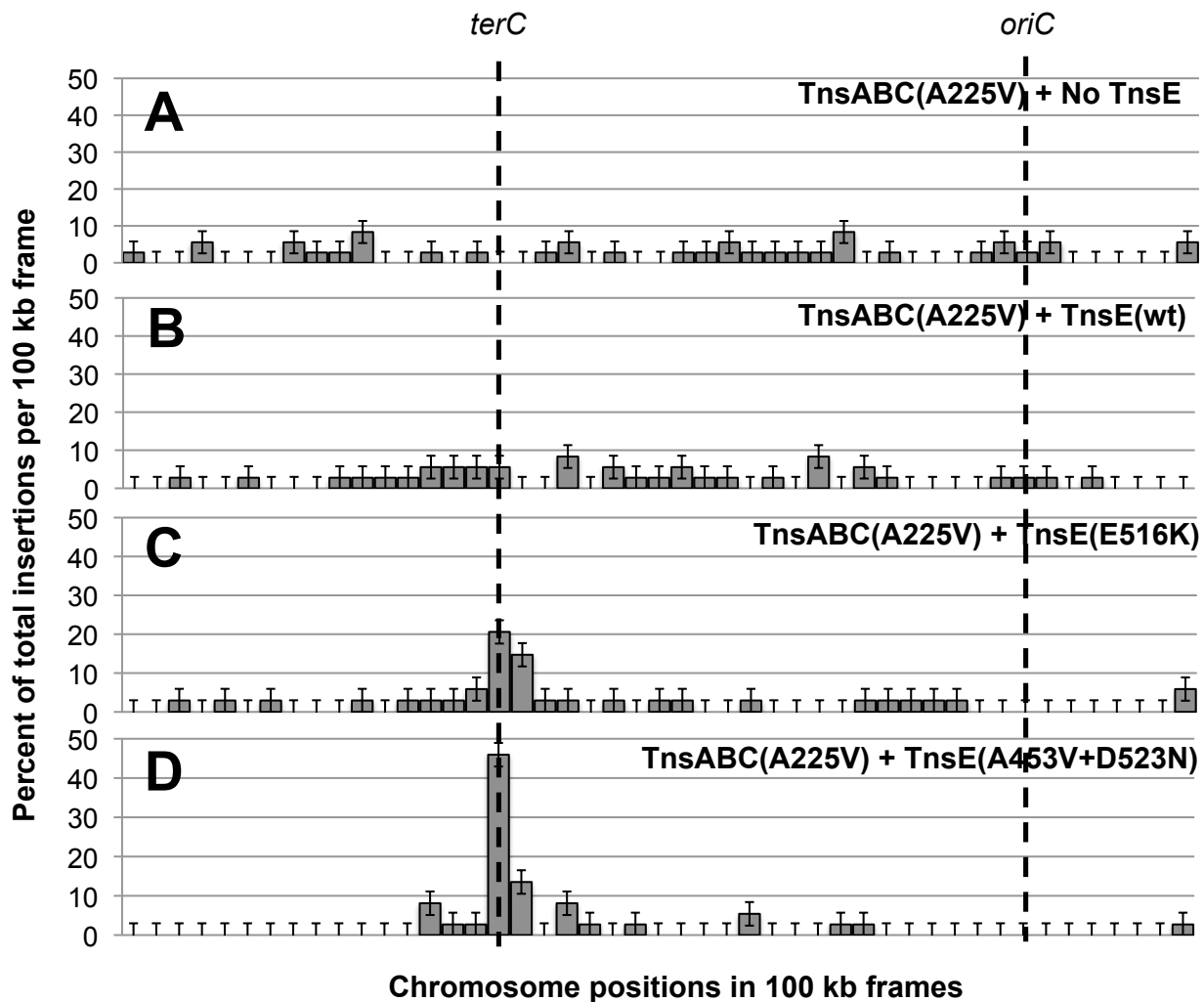
Orthogonal views of the asymmetric unit of the TnsE-CTD crystals. The twelve copies contained in the asymmetric unit are organized into two pseudo trimers of dimers. Equivalent dimers on the crystallographic oligomers are colored in light and dark shades of orange, blue and green. The buried surface ranges between 528-616 Å² (dimers) and 89-165 Å² (trimers). **(B)** The dimers are held together through reciprocal interactions between residues Arg420 and Arg422 in the $\beta 1\beta 2$ loop and the $\alpha 3\alpha 4$ (residues 487-493) loop. Although the V-loop (highlighted in purple) only participates minimally to this interface, the apex of the loop (Asp455-Val457) and part of the exposed arm (Lys458-Met459) become protected from the solvent. All dimers can be superimposed pairwise with rmsd < 0.5 Å, resulting in identical packing environments of the V-loop for the 12 copies of the asymmetric unit.



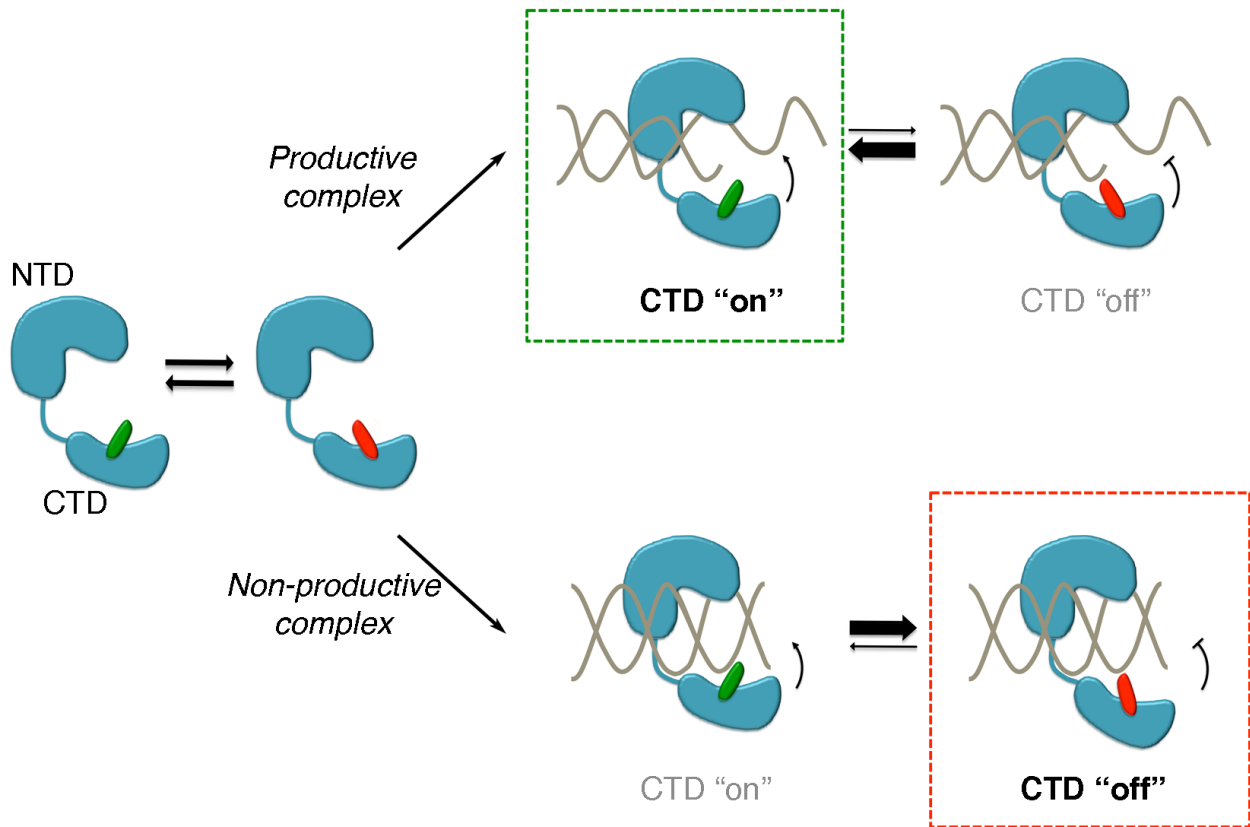
Supplementary Figure S6: Molecular replacement and composite omit map of the TnsE-CTD^{AVDN} structure. (A) Detailed view of the 2Fo-Fc and Fo-Fc electron density maps (contoured at 1σ and 3σ , respectively) generated from the molecular replacement solution obtained using the TnsE-CTD structure lacking residues Lys457-Ser461 of the V-loop. The search model is shown as color-coded sticks. **(B)** Detailed view of the composite omit map (contoured at 1.5σ) of the same region of the structure. The final TnsE-CTD^{AVDN} model is shown as color-coded sticks and water molecules as red spheres.



Supplementary Figure S7: *In vivo* transposition activity of the A453T allele in the context of various other mutant alleles. Average transposition frequencies are noted above the bars in the graph. TnsABC were expressed in all strains from pCW15 (Experimental procedures). TnsE was expressed from pJP103 (Experimental procedures). The frequency of transposition was determined using the lambda hop assay (Experimental procedures). Frequency represents the average from three experiments where the final value is multiplied by 10⁷. Error bars indicate the standard error of the mean.



Supplementary Figure S8: Distribution of Tn7 insertions across the *E. coli* chromosome in various genetic backgrounds. Targeting data from Supplementary Figure 7 was graphed as the percentage of total insertions that occurred in each 100 kb window across the *E. coli* chromosome: (A) TnsABC^{A225V} and an empty vector (pCW15* pTA106)(from Supplementary Figure 6B), (B) TnsABC^{A225V} +TnsE^{WT} (pCW15* pJP104-TnsE^{WT})(from Supplementary Figure 6C), (C) TnsABC^{A225V} +TnsE^{E516K} (pCW15* pJP104-TnsE^{E516K})(from Supplementary Figure 6D), and (D) TnsABC^{A225V} +TnsE^{A453V+D523N} (pCW15* pJP103- TnsE^{A453V+D523N})(from Supplementary Figure 6E). The position of *oriC* and *terC* are given. Error bars indicate the change in frequency expected +/- one insertion event.



Supplementary Figure S9: Model for DNA target discrimination by TnsE. Minimally, two interactions guide the ability of TnsE to recognize the lagging-strand template during DNA replication; interaction between the TnsE-NTD with the processivity factor to tether TnsE to DNA (not shown for simplicity) and interaction with a 3' recessed end DNA substrate. We propose that only when both the N-terminal domain interacts with processivity factor and the C-terminal domain of TnsE interacts with a 3' recessed end do the two domains interact productively to signal the core TnsABC machinery to initiate transposition. As indicated in the figure, the V-shaped loop toggles between two alternate conformations (shown as green and red). We propose that only the TnsE "on" conformation signals the core transposition machinery to allow assembly of the larger TnsABC protein complex. When the 3' recessed end DNA structure that is productive for transposition is recognized, TnsE resides in the "on" conformation for a longer period of time, whereas other DNA substrates drive the V-shaped loop to spend more time in the "off" conformation. Such a mechanism would allow proofreading of DNA substrates directing transposition to only occur with the preferred substrate.

Table 1. Transposition activity in the TnsE single amino acid change mutants

TnsE Allele	TnsE Expressed with Native Promoter ^a		TnsE Expressed with <i>p/lac</i> Promoter ^b	
	Transposition Frequency x 10 ⁷	Fold increase over wild type	Transposition Frequency x 10 ⁷	Fold increase over wild type
No TnsE	0.32 (0.09) ^c	0.3	0.32 (0.09) ^c	0.0009
WT	0.96 (0.32)	1	352.77(6.75)	1
A453V	18.63 (0.97)	19	3319.86 (62.00)	9
D523N	15.9 (2.28)	17	2400.00 (11.41)	7
G483R	1.59 (0.18)	2	1146.10 (11.49)	3
G515R	3.66 (0.56)	4	2614.18 (14.61)	7
E516K	2.07 (0.40)	2	1952.48 (8.98)	6
E522K	4.30 (0.69)	5	1310.64(11.15)	4
M37I	3.35 (0.89)	4	0	NA

^a Transposition was assayed in strains expressing TnsABC (pCW15) and TnsE (pJP103).

^b Transposition was assayed in strains expressing TnsABC (pCW15) and TnsE (pJP104).

^c n=3, parenthesis indicate the standard error of the mean.

NA = Not Applicable